

Analytical Model of Temperature Field in Unsteady Stage of Friction Plug Welding

YAN Chongjing^{1*}, ZHENG Yongle²

1. College of Mechanical and Electrical Engineering, Nanjing University of Aeronautics and Astronautics, Nanjing 210016, P. R. China;

2. Shanghai Aircraft Design and Research Institute, Shanghai 201206, P. R. China

(Received 31 August 2018; revised 23 July 2019; accepted 25 September 2019)

Abstract: The temperature field in unsteady phase greatly affects the quality of friction plug welding (FPW). An analytical model is put forward to correlate the process parameters and the temperature field in unsteady phase of FPW. Applying the von Mises criterion for plastic deformation and linearizing the heat flux, the model is achieved by Laplace transformation. The predicated peak temperature and peak time agree with the experiment data, with errors of about 4% and 8%, of AA7075-T6 FPW.

Key words: friction plug welding(FPW); unsteady stage; temperature field; analytical model

CLC number: TG453 **Document code:** A **Article ID:** 1005-1120(2019)05-0789-09

0 Introduction

Friction welding utilizes the relative motion between the contact surfaces of the workpieces being welded to generate frictional heat and plastic deformation on the friction surface, and increases the temperature around the welding surface to $0.6\text{--}0.9T_m$ (melting point). Due to the high pressure and the plastic deformation at the interface, joint is achieved through atomic diffusion and recrystallization^[1]. Friction plug welding (FPW), as a variation of friction welding, is a process of filling pre-drilled hole with a tapered plug. It can be used in defects removing of aluminum alloys and magnesium alloys. Thus it finds a wide application in aerospace manufacturing^[2-4].

It is believed that the formation of welded joints mainly depends on the steady stage and the upset stage. At the same time, scholars focus on heat production and temperature field of the steady stage, which are independent with the friction time. Sellars and Tegart^[5] proposed, and modified by Sheppard and Wright^[6] subsequently, the constitu-

tive equation of inverse hyperbolic sine function to model the plastic behavior in friction welding. To simplify the coupling of the temperature and the large strain rate in friction welding, methods^[7-9] are proposed to get reliable constants. The equation is widely used to calculate the thickness of plastic region, average temperature and temperature profile^[10-14].

However, experiments implying upset stage is not necessarily required for friction welding. Kimura et al.^[15] even suggested that friction welding of carbon steel could be successfully conducted without a steady stage. In this point of view, the friction heat production in unsteady stage is critical to friction welding.

More complicated than the steady stage, the unsteady stage only accounts for 10%^[16] of the total heat generation. Therefore, it is usually be simplified by Coulomb friction with a constant coefficient of friction^[17-20]. Considering the sliding-sticking mechanism of the interface, a state variable δ , which denotes the extent of sticking, is introduced to solve the interfacial heat generation problem^[21].

*Corresponding author, E-mail address: yancj@nuaa.edu.cn.

How to cite this article: YAN Chongjing, ZHENG Yongle. Analytical Model of Temperature Field in Unsteady Stage of Friction Plug Welding[J]. Transactions of Nanjing University of Aeronautics and Astronautics, 2019, 36(5): 789-797.

<http://dx.doi.org/10.16356/j.1005-1120.2019.05.010>

However, the evolution of the variable δ is unknown, which results in the difficulty of calculating the temperature field.

This paper establishes a simple analytical model that can clearly reveal the relationship between the temperature field and the process parameters, and accurately describes the distribution of temperature during unsteady stage FPW. With the linearized heat flux and Laplace transformation, the established model can predicate the temperature field of the unsteady stage of FPW covering the process parameters including the rotational speed and the friction pressure. The model is evaluated by systematically comparing the calculated results with the experimental data of 7075-T6 aluminum alloy FPW.

1 Peak Temperature

The end of the unsteady stage is the moment when the material at interface is completely plasticized. After that the mechanism of the heat generation fundamentally changed from friction heat to plastic dissipation. Therefore, it is necessary to analyze the physical mechanism of the interface friction mechanism.

Referring to the plastic forming, plastic deformation occurs only when the equivalent stress of material exceeds the yield strength of material. Its expression is as follows

$$\sigma_e \geq \sigma_s(T) \quad (1)$$

where σ_e and $\sigma_s(T)$ are the effective stress and yield strength of the material at temperature T , respectively. As shown in Fig.1, the effective stress σ_e can be expressed as follows

$$\sigma_e = \sqrt{P^2 + 3\tau^2} \quad (2)$$

where τ and P are the friction shear stress and the

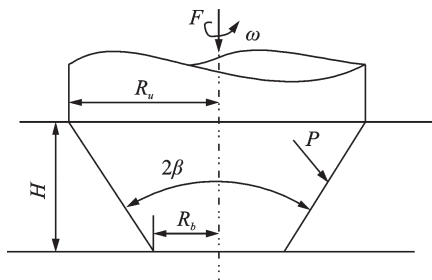


Fig.1 Interface of FPW

normal pressure at the interface, respectively. $P = F / [\pi(R_u^2 - R_b^2)]$, in which F is the axial force.

Sliding dominates the heat generation before the material yields. Consequently, the friction shear stress is calculated as

$$\tau = fP \quad (3)$$

Substituting Eq.(3) into Eq.(2), the effective stress σ_e becomes

$$\sigma_e = P\sqrt{1 + 3f^2} \quad (4)$$

Derived from the trilogy, the coefficient of friction in unsteady stage of friction welding can be expressed as^[22]

$$f = aP^b T^c e^{dv_t} \quad (5)$$

where a , b , c and d are constants to be determined by regression, and $v_t = \omega(R_u + R_b)/2$ is friction velocity, here ω is the angular speed of the plug.

Hence the peak temperature is obtained by solving the combination of Eqs.(1), (4) and (5).

2 Analytical Model of Temperature Field

2.1 Hypotheses

The analytical model is developed to simplify the mathematical description based on the following assumptions.

(1) During the FPW process, the rotational speed and the welding pressure (i.e. axial pressure) are considered to be a constant.

(2) Temperature gradient, stress, strain and width of the plastic region are uniform along the sheet thickness due to small thickness and taper angle.

(3) The weld region in the steady stage nearby the contact interface is divided into the plastic region and the elastic region, illustrated in Fig.2.

(4) Stress, strain rate, velocity of plastic flow

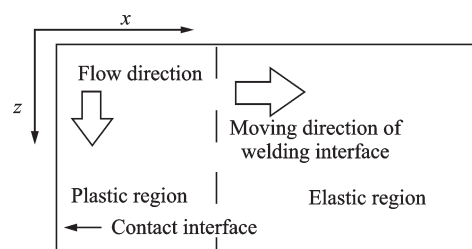


Fig.2 Weld regions

are symmetric with respect to the interface because of the identical material and heat distribution on both sides.

(5) Convection and radiation are ignored.

(6) The visco-plastic material flow in the steady stage is considered as a non-Newtonian, incompressible laminar flow.

(7) Material properties are constant.

2.2 Linearization of heat input power

Based on the first and the second hypotheses, it can be seen that the FPW process, whether the steady-state or the unsteady phase can be simplified as a 1D model problem.

In the Cartesian coordinate system, as shown in Fig.3, the contact interface, the plastic-elastic region interface, and the sheet end are set at $x = 0$, $x = B$ and $x = L$, respectively. Figs.3(a, b) schematically illustrate the temperature and flow velocity profile, respectively.

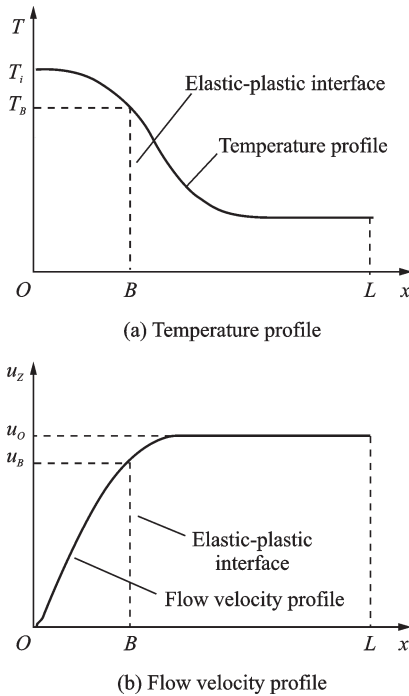


Fig.3 Schematic illustration of temperature profil and flow velocity profile

The continuity equation for incompressible single-phase flow is given by^[11]

$$\frac{\partial u_i}{\partial x_i} = 0 \quad (6)$$

where u is the velocity of plastic flow, $i = 1$, representing the x direction in Fig.3. The steady single

phase momentum conservation equation is given by^[11-12]

$$\rho \frac{\partial u_i u_j}{\partial x_i} = -\frac{\partial p}{\partial x_j} + \mu \frac{\partial}{\partial x_i} \left(\frac{\partial u_j}{\partial x_i} + \frac{\partial u_i}{\partial x_j} \right) - \rho v_M \frac{\partial u_i}{\partial x_i} \quad (7)$$

where $j=2$ or 3 , representing y and z directions in Fig.3; ρ is the density, μ the non-Newtonian viscosity, v_M the moving velocity of welding interface, and p the pressure exerted on the plastic flow parallel to the flow direction.

During the FPW process, the moving velocity of welding interface v_M is usually much less than the linear velocity of the rotating plug. Hence, v_M , u_x , and u_y in Eq.(7) can be neglected^[14]. So the equation is simplified to the following form

$$-\frac{\partial p}{\partial z} + \frac{\partial}{\partial x} \left(\mu \frac{\partial u}{\partial x} \right) = 0 \quad (8)$$

where u is u_x . Using the Perzyna visco-plastic model^[15], μ can be expressed as

$$\mu = \frac{\sigma_e}{3\dot{\epsilon}} \quad (9)$$

where $\dot{\epsilon}$ is the effective strain rate.

The effective strain rate is given by

$$\dot{\epsilon} = \frac{1}{\sqrt{3}} \left(\frac{\partial u}{\partial x} \right) \quad (10)$$

Substituting Eqs.(9) and (10) into Eq.(8) and integrating Eq.(8) and combining with the boundary condition $\sigma_e = \tau(T_B)$ at $x=B$, σ_e can be written as

$$\sigma_e = \sqrt{3} \frac{\partial p}{\partial z} (B-x) + \tau(T_B) \quad (11)$$

For the material enduring high temperature and high strain rate, Sheppard and Wright^[6] proposed a constitutive equation

$$\sigma_e = \frac{1}{\alpha} \sinh^{-1} \left[(Z/A)^{1/n} \right] \quad (12)$$

where A , α and n are the material parameters, and Z is the Zener - Hollomon parameter, which is given by

$$Z = \dot{\epsilon} \exp \left(\frac{\Delta H}{GT} \right) \quad (13)$$

where G is the universal gas constant, ΔH the activation energy, and T the Kelvin temperature.

An equation for u can be derived from Eq.(11), and taking Eqs.(12) and (13) into account, it is expressed as

$$\sinh^{-1}\left(\frac{Z}{A}\right)^{\frac{1}{n}} = \sinh^{-1}\left(\frac{1}{\sqrt{3}} \frac{\partial u}{\partial x} e^{\frac{\Delta H}{GT}}\right)^{\frac{1}{n}} = \sqrt{3} \alpha \frac{\partial p}{\partial z} (B-x) + \tau(T_B) \quad (14)$$

In order to solve the velocity u , Aukrust et al.^[13] proposed a simplified method that the function $\sinh^{-1}x$ is approximately equal to the logarithm function $\ln 2x$ when x is larger than 1. Xiong, Qian et al.^[10,12] stated that the requirement $(Z/A)^{1/n} \gg 1$ is met during the plastic flow of friction stir welding (FSW) and continuous drive friction welding (CDFW). Thus it is reasonable to assume that the plastic flow region of FPW also satisfies the condition. Hence, Eq.(14) can be simplified as

$$\sinh^{-1}\left(\frac{Z}{A}\right)^{\frac{1}{n}} \approx \ln\left[2\left(\frac{Z}{A}\right)^{\frac{1}{n}}\right] \quad (15)$$

Although the temperature gradient is large, the plastic flow region is narrow (<1 mm), resulting in a small temperature difference across the region, about ten to dozens degrees^[10]. Thus it is reasonable to substitute the T with the average temperature of the flow region T_a , and T_B can be estimated as $T_B = T_{\max} - 20$. After substituting Eq.(15) into Eq.(14), the expression for u can be obtained by integrating Eq.(14) with the boundary condition $u=0$ at $x=0$ (Fig.3(b)), and it is described as

$$u = \frac{\sqrt{3}}{2^n} \frac{A b e^{B/b + n\alpha\tau(T_B)}}{e^{\Delta H/GT_a}} (1 - e^{-x/b}) \quad (16)$$

where $b = \left(\sqrt{3} n \alpha \frac{\partial p}{\partial z}\right)^{-1}$.

Differentiating Eq.(16) and substituting it into Eq.(10), the effective strain rate is acquired as

$$\dot{\epsilon} = A \exp\left(\frac{B}{b + n\alpha\tau(T_B)} - \frac{x}{b} - \frac{\Delta H}{GT_a}\right) \quad (17)$$

As shown in Eqs.(16) and (17), the effective strain rate and the velocity rapidly decrease with x increasing from 0 to b . While it decreases slowly when x increases from b to L . Thus the location $x=b$ can be defined as the plastic flow/deform interface, i.e. the variable b can represent the thickness of the plastic region B

$$B = b = \left(\sqrt{3} n \alpha \frac{\partial p}{\partial z}\right)^{-1} \quad (18)$$

Based on the definition of B in Eq.(18) and considering Eq.(11), the flow stress σ_e can be expressed as

$$\sigma_e = \frac{B-x}{n\alpha B} + \tau(T_B) \quad (19)$$

Substituting Eq.(18) into Eq.(17), the effective strain rate in FPW can be expressed as

$$\dot{\epsilon} = \frac{1}{2^n} A \exp\left(n\alpha\tau(T_B) + 1 - \frac{x}{B} - \frac{\Delta H}{GT_a}\right) \quad (20)$$

The material velocity at position $x=B/2$ can be assume to be $v/2$ ^[10], and v is half of the rotation speed. Then according to Eqs.(16) and (18), $v_{x=B/2}$ yields

$$v_{x=B/2} = \frac{v}{2} = \frac{\sqrt{3}}{2^n} \frac{A B e^{n\alpha\tau(T_B) + 1}}{e^{\Delta H/GT_a}} (1 - e^{-1/2}) \quad (21)$$

and

$$\dot{\epsilon} = \frac{1}{2\sqrt{3}} \frac{v}{(1 - e^{-1/2})} \frac{v}{B} \exp\left(-\frac{x}{B}\right) \quad (22)$$

The heat generation rate for plastic deformation of material within a unit volume is given by

$$q = \eta \sigma_e \dot{\epsilon} q \quad (23)$$

where η is the efficiency of conversion of plastic strain energy into heat energy. Thus, the heat production of the plastic zone of volume V can be expressed as

$$P = \int_V \eta \sigma_e \dot{\epsilon} dV \quad (24)$$

Considering $\eta = 1$, the heat generation of the entire plastic region is equal to the welding power P_w . Therefore

$$P_w = P_{B_1} + P_{B_2} \quad (25)$$

where P_{B_1} and P_{B_2} are the heat generation of the plastic region in substrate and that in plug, respectively.

Since the thickness of plastic region in both sides of the interface is equal, $P_{B_1} = P_{B_2}$

$$P_w = \frac{2(1 + e^{\frac{1}{2}} \pi R H v \tau(T_B))}{\sqrt{3}} \quad (26)$$

where $R = (R_a + R_b)/2$.

In the study of friction plug welding, the friction torque profile of unsteady stage increases approximately linearly. That is, the heat power increases lin-

early from 0 to peak value. Li^[23] proposed the linear hypothesis for heat flux of the unsteady stage of rotary friction welding. The hypothesis is supported by Luo^[24]. Therefore, the linear hypothesis for heat intensity can be applied to the unsteady stage of FPW, and accordingly the heat flux can be written as

$$q(t) = \frac{P_w}{St_p} \cdot t = Ct \tag{27}$$

where t_p is the elapsed time to peak torque, as well as the duration of unsteady stage, S the area of the welding interface, and C the constant

$$C = \frac{2(1 + e^{-\frac{1}{2}})v\tau(T_B)\cos\beta}{\sqrt{3}t_p} \tag{28}$$

2.3 Temperature field

Calculating the unsteady stage temperature field of FPW is a typical transient heat conduction problem, without internal heat source. Thus, the governing equation of transient temperature field $T(x, t)$ is given by

$$\frac{\partial T}{\partial t} = \kappa \frac{\partial^2 T}{\partial x^2} \quad 0 < x < \infty, t > 0 \tag{29a}$$

where T is the temperature (K) that changes with time t and position x , and κ the thermal diffusion coefficient ($m^2 \cdot s^{-1}$).

According to the Fourier law of heat conduction and the heat flux linearization hypothesis proposed in section 2.2, Eq. (29a) with Neumann boundary condition is given by

$$\lambda \frac{\partial T}{\partial x} = -Ct \quad x = 0, t > 0 \tag{29b}$$

When steady stage is considered, Eq. (29a) should also satisfy Dirichlet boundary condition and be written as

$$T(x, t) = T_0 \quad x \rightarrow \infty, t > 0 \tag{29c}$$

$$T(x, t) = T_0 \quad x \geq 0, t = 0 \tag{29d}$$

where T_0 is the ambient temperature. It is also the initial temperature for FPW.

Performing Laplace transform on t , Eqs.(29a)—(29c) yield

$$\frac{d^2 \bar{T}(x, s)}{dx^2} - \frac{s}{\kappa} \bar{T}(x, s) = 0 \quad 0 < x < \infty \tag{30a}$$

$$\frac{d\bar{T}(x, s)}{dx} = -\frac{C}{\lambda} \frac{1}{s^2} \quad x = 0 \tag{30b}$$

$$\bar{T}(x, s) = \frac{T_0}{s} \quad x \rightarrow \infty \tag{30c}$$

The Laplace transformation of the temperature distribution can be obtained by integrating Eq.(30a) with the boundary conditions and yields

$$\begin{aligned} \bar{T}(x, s) &= \frac{C}{\lambda} \frac{1}{s^2} \sqrt{\frac{k}{s}} e^{-x\sqrt{\frac{s}{k}}} + \frac{T_0}{s} = \\ &F(s)G(x, s) + \frac{T_0}{s} \end{aligned} \tag{31}$$

where $F(s) = \frac{C}{\lambda} \frac{1}{s^2}$, and $G(x, s) = \frac{e^{-x\sqrt{s/k}}}{\sqrt{\kappa/s}}$.

Giving $f(t)$ and $g(x, t)$ as the inverse Laplace transform of $F(s)$ and $G(x, s)$, and let $f(t) = C/\lambda \cdot t$, $g(x, t)$ is given by

$$g(x, t) = \sqrt{\frac{\kappa}{\pi t}} e^{-x^2/4\kappa t} \tag{32}$$

Based on the convolution theorem, Eq. (31) can be written as

$$T(x, t) - T_0 = \frac{C\sqrt{\kappa}}{\lambda\sqrt{\pi}} \int_0^t \frac{t-\tau}{\sqrt{\tau}} e^{-\frac{x^2}{4\kappa\tau}} d\tau \tag{33}$$

With variable substitution and integration

$$\frac{x}{2\sqrt{\kappa\tau}} = z \rightarrow \tau = \frac{x^2}{4\kappa z^2} \rightarrow d\tau = -\frac{x^2}{2\kappa z^3} dz \tag{34}$$

It yields

$$\begin{aligned} T(x, t) &= T_0 + \frac{C}{3\lambda k \sqrt{\pi}} e^{\frac{x^2}{4\kappa t}} \sqrt{\kappa t} (x^2 + 4\kappa t) - \\ &\frac{C}{6\lambda k \sqrt{\pi}} x(x^2 + 6\kappa t) \operatorname{erfc}\left(\frac{x}{2\sqrt{\kappa t}}\right) \end{aligned} \tag{35}$$

3 Experimental and Analytical Solution

3.1 Experiment

The FPW of AA7075-T6 was carried out to systematically evaluate the analytical solution. The chemical composition of AA7075-T6 is shown in Table 1 and the specific values of the parameters involved are given in Table 2.

Tools used for experiment is a self-made set-

Table 1 Chemical composition of A7075-T6

Element	Mg	Cu	Fe	Si	Mn	Ti	Other	Al
Content/%	5.1—6.1	2.1—2.9	≤0.5	≤0.4	≤0.3	≤0.2	5.1—6.1	Bal.

Table 2 Structural and material properties and welding parameters

Parameter	Value	Parameter	Value
R_b /mm	5	Thermal conductivity λ /($\text{W}\cdot\text{m}^{-1}\cdot\text{K}^{-1}$)	130
Dimension of specimen /($\text{mm}\times\text{mm}\times\text{mm}$)	100×40×4	Heat capacity J /($\text{kg}\cdot\text{K}^{-1}$)	960
Angle of tapered hole, β /($^\circ$)	25	Material parameter n ^[7]	6.5
Thermal diffusivity κ /($\text{m}^2\cdot\text{s}^{-1}$)	4.8×10^{-5}	Material parameter α ^[7]	0.012
Rotation speed n /($10^3\cdot\text{r}\cdot\text{min}^{-1}$)	3/3.2/3.5/3.8/4	Activation energy ΔH /($\text{kJ}\cdot\text{mol}^{-1}$) ^[25-26]	160
Friction pressure P /MPa	14/16/18/20/22	Gas constant G /($\text{J}\cdot\text{mol}^{-1}\cdot\text{K}^{-1}$)	8.314

up, with rotation speed of 0—5 000 r/min, feed rate of 0—4 mm/s, clamp diameter of 0—20 mm. Specimen is fixed on a supporting plate, of 45 steel, by a universal fixture. The end of the plug has the same shape and dimension as the hole. Thermocouples are buried in the pre-drilled holes, centered at the sheet section, and adjacent to the contact surface with 1 mm distance. Temperature of these points are taken as that of the contact surface due to the small distance and high thermal conductivity of aluminum alloy.

Since the friction pressure P and rotational speed n are both important welding parameters, two sets of experiments were set up. The experiment uses a simple exposed thermocouple to quickly acquire the evolution of the temperature field. In the first set of experiments, P was increasing from 14 MPa to 22 MPa with a constant n of 3 500 r/min. The second set of experiments was conducted by changing n from 3 000 r/min to 4 000 r/min with a constant P of 20 MPa.

With the data, in Table 3, acquired from FPW experiment, the friction coefficient of 7075-T6 is regressed as follows

$$f = 51.924P^{-0.647}(T - 273)^{-0.172}e^{-0.632v_t} \quad (36)$$

Scope of application: 7075-T6 Al alloy, $P=14\text{--}31$ MPa, $T=372\text{--}720$ K, $v_t=1.869\text{--}2.605$ m/s.

As shown in Fig.4, the yield strength of 7075-T6 aluminum alloy varies significantly with temperature^[27]. The relation between yield strength and temperature ($T \geq 373$ K) is fitted as the following formula

$$\sigma_s = 433.77e^{-\frac{T}{2131.84}} + 2181850e^{-\frac{T}{42.98}} - 287 \quad (37)$$

Table 3 Experiment data for regression of friction coefficient of A7075-T6

P /MPa	T /K	v_t /($\text{m}\cdot\text{s}^{-1}$)	f	P /MPa	T /K	v_t /($\text{m}\cdot\text{s}^{-1}$)	f
22	480	1.869	0.866	14	720	2.181	0.624
25.5	512	1.869	0.756	22	446	2.181	0.734
23	579	1.869	0.772	31	483	2.181	0.559
30	621	1.869	0.649	25	631	2.181	0.597
15	372	2.605	0.782	21	668	2.181	0.650
31	486	2.605	0.447	20	524	2.181	0.722
28	525	2.605	0.448	14	576	2.181	0.905
14	575	2.605	0.651	21	429	2.181	0.762
25	649	2.605	0.445	25	492	2.181	0.658

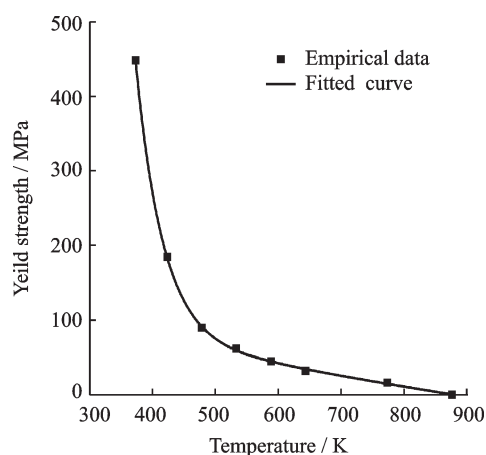


Fig.4 Variable yield stress of 7075-T6 alloy

3.2 Peak temperature

The peak temperature T_{\max} of FPW process has a great effect on the micro-structure of the joint. It can be calculated from Eqs.(1), (2), (6) and (7).

Comparison of the calculated result and experimental data is shown in Fig.5. It can be seen that the calculated result is around 20 K higher than the experimental data. The error amounts 4% of the experimental data. Causes for the error may refer to heat sink of the backing plate, which is ignored during the modeling. In addition, temperature gradient

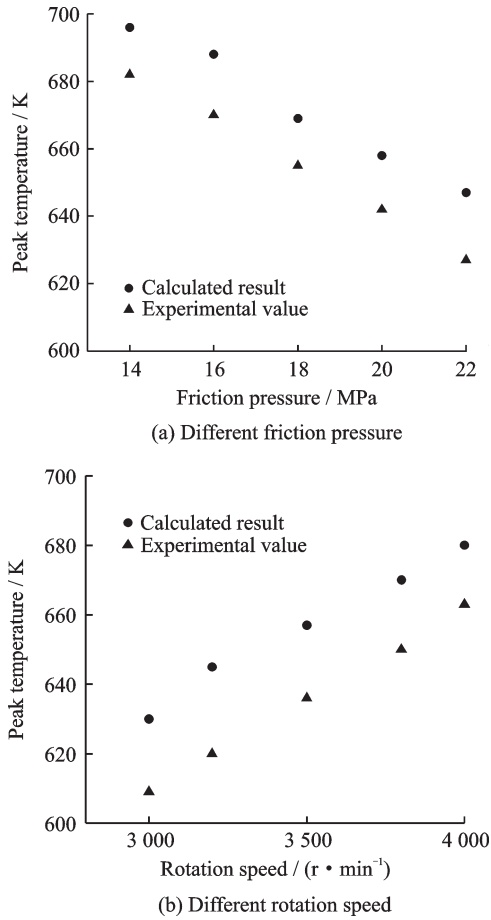


Fig.5 The peak temperature with different friction pressure and different rotation speed

between the contact surface and the measuring point should be related^[12]. However, it should be noted that the trend of the calculated curve and the experiment curve are the same. The temperature rises with pressure increases, while falls when rotation speed increases.

3.3 Elapsed time to peak torque

The elapsed time to peak torque partly determines the welding cycle. Considering the boundary condition $T = T_{max}$ at $x = 0$ and $t = t_p$, the elapsed time to peak torque can be obtained from Eq. (35) and be written as

$$t_p = \left(\frac{3\sqrt{3} \lambda \sqrt{\pi} (T_{max} - T_0)}{10.16\sqrt{\kappa} \nu \tau (T_B) \cos\beta (1 - e^{-1})} \right)^2 \quad (38)$$

Although there are errors around 0.05 s, amounting 8%, the trend of two curves are the same in Fig.6. One of the causes for the error is a constant area of contact surface, which varies during the practical welding. Besides that materials

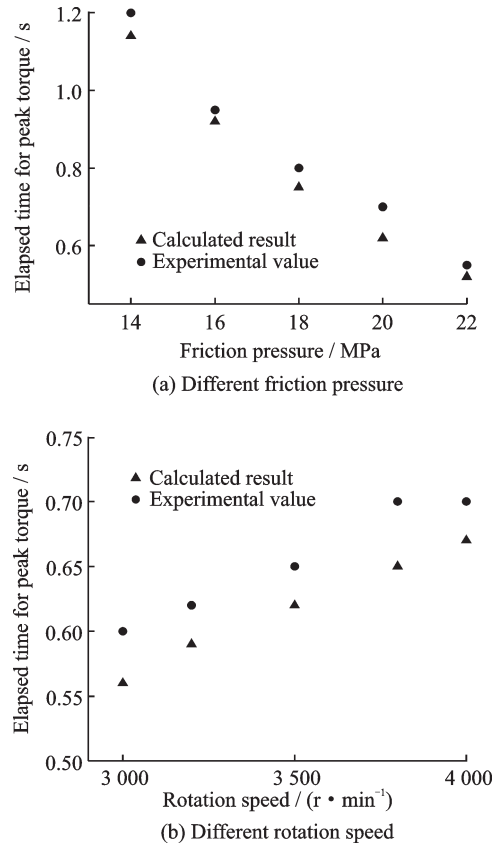


Fig.6 Elapsed time for peak torque with different friction pressure and different rotation speed

property is also a cause. The last one is the measuring error.

3.4 Temperature profile of unsteady stage of FPW

Temperature at the contact interface is chosen to evaluate the analytical model. Derived from Eq. (35), the temperature profile $T(x=0, t)$ can be described as

$$T(0, t) = \frac{10.16V \sqrt{\kappa} \tau (T_B) (1 - e^{-1}) \cos\alpha}{3\sqrt{3} t_p \lambda \sqrt{\pi}} t^{1.5} + T_0 \quad (39)$$

It can be seen in Fig.7 that the calculated results are slightly higher than the experimental data in the initial period. This is due to the fact that the real contact area is smaller than that applied to computation. Energy of friction is consumed for the destroying of oxide layer until the fresh surface exposed completely. So there is a flatness of experimental data curve in the initial period. After that friction heat accumulates and temperature rises sharply. As temperature goes up, the slope of the

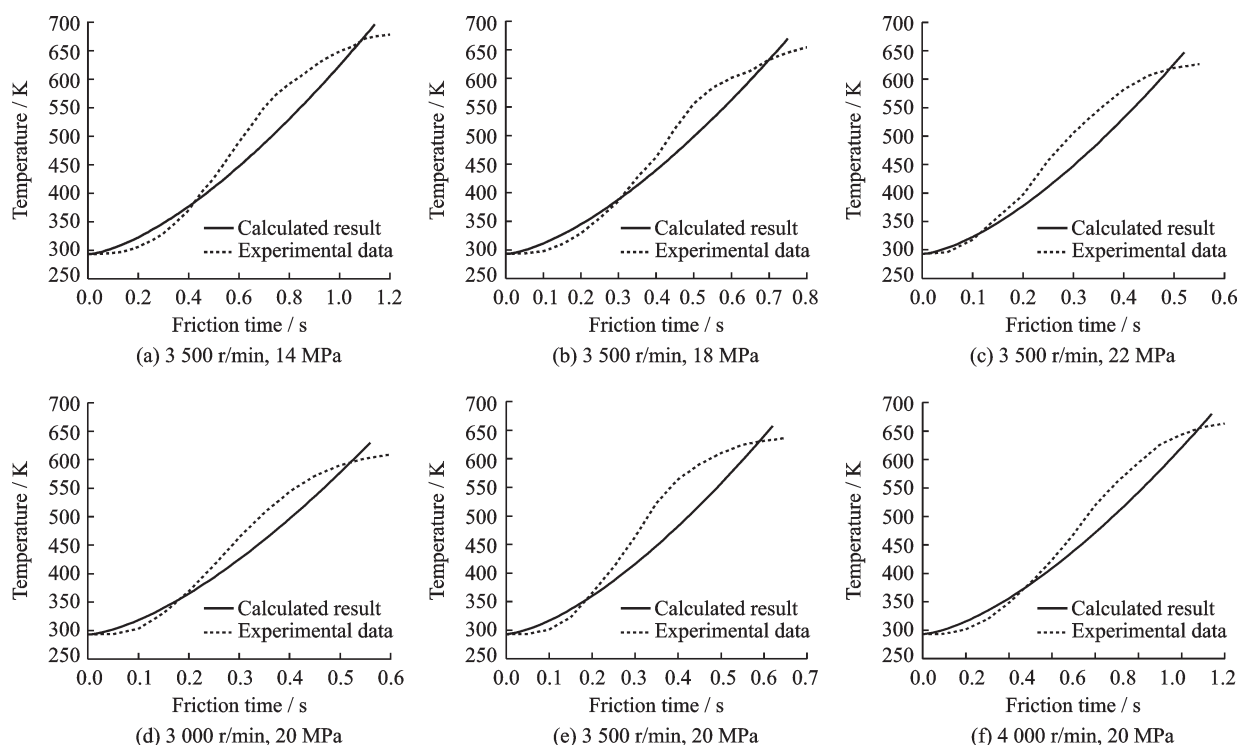


Fig. 7 Temperature profile with different rotation speeds and friction pressures during the 1st stage of FPW process

curve decreases, because of the softening of the material. In addition, analytical model neglected the softening in high temperature by applying constant value of material properties and friction coefficient. Despite some differences, the general trend of analytical curve and experiment curve is the same.

4 Conclusions

(1) An analytical thermal model is proposed for the unsteady stage of A7075-T6 FPW. In this model, the coefficient of friction is regressed and the elapsed time for peak torque is derived from the temperature field.

(2) Linear heat flux is a reasonable assumption for the unsteady stage of FPW, though errors become larger when the temperature approaches the peak value.

References

- [1] KEVIN J G. Friction welding takes on new applications[J]. *Welding Journal*, 1997(9): 39-40.
- [2] RICHARD F. Bringing aerospace welding specifications up to standard[J]. *Welding and Metal Fabrication*, 2000, 68(7): 12-14.
- [3] DELANY F, LUCAS W, THOMAS W, et al. Advanced joining processes for repair in nuclear power plants[C]// *Proceedings of 2005 International Forum on Welding Technologies in Energy Engineering*. Shanghai, China: [s. n.], 2005: 54-69.
- [4] LEI X F, DENG Y, YIN Z M, et al. Tungsten inert gas and friction stir welding characteristics of 4-mm-Thick 2219-T87 plates at room temperature and -196 °C[J]. *ASM International*, 2014: 2149-2158.
- [5] SELLARS C M, TEGART W J. Hot workability[J]. *Int Met Rev*, 1972, 17: 1-24.
- [6] SHEPPARD T, WRIGHT D S. Determination of flow stress: Part 1 constitutive equation for aluminum alloys at elevated temperatures[J]. *Met Technol*, 1979, 16: 215-223.
- [7] SHEPPARD T, JACKSON A. Constitutive equations for use in prediction of flow stress during extrusion of aluminum alloys[J]. *Materials Science and Technology*, 1997, 13: 203-209.
- [8] PRASAD Y, SESHACHARYULU T, MADEIROS S, et al. Hot deformation mechanisms in Ti-6Al-4V with transformed β starting microstructure commercial v. extra low interstitial grade[J]. *Materials Science and Technology*, 2000, 16: 1029-1036.
- [9] TELLO K E, GERLICH A P, MENDEZ P F. Constants for hot deformation constitutive models for recent experimental data[J]. *Science and Technology of Welding and Joining*, 2010, 15(3): 260-266.
- [10] XIONG J T, LI J L, WEI Y N, et al. An analytical

- model of steady-state continuous drive friction welding[J]. *Acta Materialia*, 2013, 61: 1662-1675.
- [11] NANDAN R, ROY G G, LIENERT T J, et al. Three-dimensional heat and material flow during friction stir welding of mild steel[J]. *Acta Materialia*, 2007, 55: 883-895.
- [12] QIAN J W, OU Y, LI J L, et al. An analytical model to calculate the peak temperature for friction stir welding[J]. *Science and Technology of Welding and Joining*, 2017, 22(6): 520-525.
- [13] AUKRUST T, LAZGHAB S. Thin shear boundary layers inflow of hot aluminum[J]. *International Journal of Plasticity*, 2000, 16: 59-71.
- [14] MENDEZ P F, TELLO K E, LIENERT T J. Scaling of coupled heat transfer and plastic deformation around the pin in friction stir welding[J]. *Acta Materialia*, 2010, 58: 6012-6026.
- [15] KIMURA M, INOUE H, KUSAKA M, et al. Analysis method of friction torque and weld interface temperature during friction process of steel friction welding[J]. *Journal of Solid Mechanics and Materials Engineering*, 2010, 4: 401-413.
- [16] VILL V I. Friction welding of metals[M]. American Welding Society, Trade Distributor: Reinhold Pub Co, 1962: 27-33.
- [17] RYKALIN N N, PUGIN A I, VASIL E. The heating and cooling of rods butt-welded by the friction process[J]. *Welding Production*, 1959: 42-52.
- [18] MIDLING O T, GRONG Ø. A process model for friction welding of Al-Mg-Si alloys and Al-Si C metal matrix composites-I. Haz temperature and strain rate distribution[J]. *Acta Metallurgica et Materialia*, 1994, 42(5): 1595-1609.
- [19] VAIRIS A, FROST M. Modelling the linear friction welding of titanium blocks[J]. *Materials Science and Engineering A*, 2000, 292(1): 8-17.
- [20] AMBROZIAK A, WINNICKI M, LASKA P, et al. Examination of friction coefficient in friction welding process of tubular steel elements[J]. *Archives of Metallurgy and Materials*, 2011, 56(4): 975-980.
- [21] MAALEKIAN M, KOZESCHNIK E, BRANTNER H P, et al. Comparative analysis of heat generation in friction welding of steel bars[J]. *Acta Materialia*, 2008, 56(12): 2843-2855.
- [22] DU Suigeng, DUAN Liyu, WU Shidun, et al. The friction mechanism and friction coefficient at the initial stage of friction welding[J]. *Mechanical Science and Technology*, 1997, 16(4): 704-706. (in Chinese)
- [23] LI Peng. Heat source evolution and joint formation in rotary friction welding process[D]. Xi'an: Northwestern Polytechnical University, 2015. (in Chinese)
- [24] LUO J. New measurement technique and model for friction torque in continuous driven friction welding: Engineering oriented voltage-current floating evaluation measurement method and exponential function model of friction torque[J]. *Science and Technology of Welding and Joining*, 2001, 6(4): 209-212.
- [25] HUANG Y X, XIE Y M, MENG X C, et al. Numerical design of high depth-to-width ratio friction stir welding[J]. *Journal of Materials Processing Technology*, 2018, 252: 233-241.
- [26] HU S, WU C S, PITTNER A, et al. Thermal energy generation and distribution in friction stir welding of aluminum alloys[J]. *Energy*, 2014, 77: 720-731.
- [27] PAN Fusheng, ZHANG Dingfei. Aluminum alloy and application[M]. Beijing: Chemical Industry Press, 2006. (in Chinese)
- Authors** Dr. YAN Chongjing received the Ph.D. degree in mechanical engineering from Nanjing University of Aeronautics and Astronautics in 2009 and worked there till now. The main focus of his research is related to friction welding and relevant fields.
- Mr. Zheng Yongle received the M.S. degree in mechanical engineering from Nanjing University of Aeronautics and Astronautics in 2019. His research is related to big data analysis.
- Author contributions** Dr. YAN Chongjing designed the study, compiled the models, conducted the analysis, interpreted the results and wrote the manuscript. Mr. ZHENG Yongle contributed data, coefficient of friction regression and plots for the mathematical model. All authors commented on the manuscript draft and approved the submission.
- Competing interests** The authors declare no competing interests.

(Production Editor: Xu Chengting)